Large Zero-Field Cooled Exchange-Bias in Bulk Mn_2PtGa

A. K. Nayak,[1,*] M. Nicklas,[1,†] S. Chadov,[1] C. Shekhar,[1] Y. Skourski,[2] J. Winterlik,[3] and C. Felser[1,3]

[1]*Max Planck Institute for Chemical Physics of Solids, Nöthnitzer Strasse 40, D-01187 Dresden, Germany*

[2]*Dresden High Magnetic Field Laboratory (HLD), Helmholtz-Zentrum Dresden-Rossendorf, D-01328 Dresden, Germany*

[3]*Institut für Anorganische und Analytische Chemie, Johannes Gutenberg-Universität, 55099 Mainz, Germany*

(Received 30 July 2012; revised manuscript received 11 December 2012; published 19 March 2013)

We report a large exchange-bias effect after zero-field cooling the new tetragonal Heusler compound Mn_2PtGa from the paramagnetic state. The first-principles calculation and the magnetic measurements reveal that Mn_2PtGa orders ferrimagnetically with some ferromagnetic inclusions. We show that ferrimagnetic ordering is essential to isothermally induce the exchange anisotropy needed for the zero-field cooled exchange bias during the virgin magnetization process. The complex magnetic behavior at low temperatures is characterized by the coexistence of a field-induced irreversible magnetic behavior and a spin-glass-like phase. The field-induced irreversibility originates from an unusual first-order ferrimagnetic to antiferromagnetic transition, whereas the spin-glass-like state forms due to the existence of antisite disorder intrinsic to the material.

DOI: 10.1103/PhysRevLett.110.127204 PACS numbers: 75.60.Ej, 72.15.Jf, 75.30.Gw, 75.50.Cc

The class of $Ni_2Mn_{1+x}Z_{1-x}$ based Heusler alloys exhibit a structural transition from a high temperature cubic austenite phase to a low temperature tetragonal or orthorhombic martensitic phase, whereas a magnetic ordering transition takes place in the cubic phase. The existence of a first-order structural transition with strong magnetostructural coupling leads to the observation of various functional properties [1–4]. In these off-stoichiometric Mn rich alloys the extra Mn replaces the Z atoms. The Mn-Mn exchange interaction is ferromagnetic (FM) within the regular Mn sublattices while it is antiferromagnetic (AFM) between the Mn atoms occupying the regular Mn sublattice and Z sublattice [5,6]. The tetragonal or orthorhombic distortion in the martensitic phase enhances this AFM interaction due to the decrease in the Mn-Mn distance, which also results in a large degree of magnetic frustration. Furthermore, many Heusler alloys also display antisite disorder [7]. All these factors contribute to a complex magnetic state in the low temperature regime. The observations of spin-glass behavior [8–10] and the exchange-bias (EB) phenomenon [8,11] are direct evidence of this complex magnetic state.

A new class of Mn_2YZ based binary and ternary Heusler compounds stabilize in the cubic or tetragonal crystal structure with high Curie temperatures (T_C). These materials are attractive candidates for spin-torque transfer devices [12–15]. The magnetic interaction in most of these compounds is found to be ferrimagnetic (FI) in nature [13,16]. The magnetic circular dichroism in x-ray absorption measurements in $Mn_{3-x}Co_xGa$ compounds shows direct evidence of the FI ordering [17]. In a recent work it is found that Mn_2PtIn, which crystallizes in a tetragonal structure with FI ordering, exhibits an inhomogeneous magnetic state at low temperature and shows a weak conventional EB effect [18]. In this Letter, we report a large unconventional EB effect obtained after zero-field cooling the Heusler compound Mn_2PtGa from its paramagnetic state. To further elucidate the microscopic origin of the EB behavior, we carried out a theoretical investigation on the magnetic structure. Based on our experimental and theoretical results, we propose a phenomenological model for the large zero-field cooled (ZFC) EB.

Polycrystalline ingots of Mn_2PtGa were prepared by arc melting stoichiometric amounts of the constituent elements and subsequent annealing for one week at 1273 K. The samples were structurally characterized by x-ray powder diffraction. The details of the structural analysis are given in the Supplemental Material [19]. The physical quantities were investigated utilizing Quantum Design measurement systems. The pulsed magnetic field experiments were performed at the Dresden High Magnetic Field Laboratory. We have also performed a calculation to map out the magnetic structure using the PYA-LMTO program package [20].

Mn_2PtGa undergoes a paramagnetic to FM (FI) transition at $T_C = 230$ K as exemplified in the magnetization $M(T)$ and ac-susceptibility $\chi(T)$ data in Figs. 1(a) and 1(b). With further decreasing temperature $M(T)$ exhibits a sudden drop at 150 K. To probe the nature of this transition we have measured field cooled (FC) and field heated (FH) $M(T)$ curves that show a significant hysteresis. The presence of such a thermal hysteresis between the FC and FH curves is a strong evidence for the first-order nature of a phase transition [21]. Therefore, we argue that Mn_2PtGa undergoes a first-order FM (FI) to AFM transition at 150 K. However, the existence of a small irreversibility between ZFC and FC curves suggests that the low temperature phase is not perfectly AFM in nature. This irreversibility mainly originates from the presence of antisite disorder that gives rise to a magnetically inhomogeneous state. We

 © 2013 American Physical Society

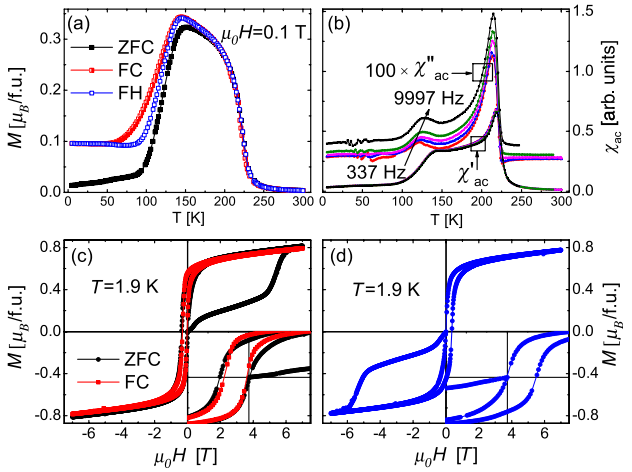

FIG. 1 (color online). (a) $M(T)$ at 0.1 T measured in ZFC, FC, and FH cycles. In the ZFC mode, the sample was initially cooled to 2 K in 0 T and data were taken upon increasing temperature in applied field. In the FC mode, data were collected while cooling in field, and subsequently in FH mode data were collected during heating. (b) Real (χ') and imaginary (χ'') part of the ac susceptibility measured with different frequencies and an amplitude of 5 Oe. (c) ZFC and FC $M(H)$ loops at 1.9 K performed as $0 \rightarrow 7 \rightarrow -7 \rightarrow 7$ T. (d) ZFC $M(H)$ loop at 1.9 K performed as $0 \rightarrow -7 \rightarrow 7 \rightarrow -7$ T. The insets show a magnified view around $H = 0$.

note that the degree of antisite disorder can be tuned by the annealing or quenching procedure. The imaginary part of the ac susceptibility $\chi''(T)$ [Fig. 1(b)] shows a maximum around 120 K which exhibits a weak frequency dependence indicating the presence of spin- or cluster-glass-like states.

Magnetization loops $M(H)$ have been measured using a ZFC or FC protocol, as indicated in Fig. 1(c). The most fascinating behavior in the ZFC $M(H)$ data is the shift of the hysteresis loop in negative field direction by about 0.17 T. To verify this effect we have measured the $M(H)$ loop also in the opposite direction [Fig. 1(d)]. As expected, this shifts by 0.17 T to the positive field direction. Therefore, we conclude that the observed EB-like behavior is intrinsic to Mn_2PtGa. Thus, it is possible to induce the exchange anisotropy by zero-field cooling from the paramagnetic state. The direction of the anisotropy field depends on the initial direction of the external field. In general, the EB effect in conventional exchange-coupled systems appears only after field cooling from a temperature above the Néel temperature of the AFM material. Thus, when the virgin $M(H)$ curve is measured in positive field direction Mn_2PtGa behaves as cooled in the presence of positive field and vice versa. The $M(H)$ loop taken at 1.9 K after field cooling in 7 T shows approximately the same shifting as the ZFC loop [see Fig. 1(c)]. Therefore, in the case of the ZFC EB, scanning the virgin magnetization process provides the roll of the cooling field required in the conventional EB systems. We note that the ZFC virgin $M(H)$ curve at 1.9 K displays a sharp magnetization change at 4.8 T, indicating a field-induced first-order metamagnetic transition from an AFM to a FI phase, which will be addressed later.

$M(H)$ measured in pulsed fields does not show any saturation up to 60 T [see Fig. 2(a)]. The sample shows a magnetization of 0.8 μ_B/f.u. in 7 T at 1.9 K and 1.6 μ_B/f.u. in 60 T at 4.2 K. The small value of the magnetization and the still increasing $M(H)$ indicate the presence of FI ordering in Mn_2PtGa. At 275 K, which is above T_C, we find paramagnetic behavior. Interestingly, the $M(H)$ curve at 4.2 K displays a similar shift to that observed in the low field ZFC $M(H)$ data. This evidences that a field of 60 T is too small to affect the exchange anisotropy produced in the sample during the initial magnetization process. The temperature dependence of the EB field (H_{EB}) and the coercive field (H_C) deduced from the ZFC and FC hysteresis loops are shown in Fig. 2(b). In FC mode the sample was cooled in 7 T from 300 K to the desired temperature. H_{EB} and H_C are calculated using $H_{EB} = |H_1 + H_2|/2$ and $H_C = |H_1 - H_2|/2$, where H_1 and H_2 are the lower and upper cutoff fields. At 1.9 K, H_{EB} possesses a maximum value of around 0.17 T in ZFC mode and 0.16 T in FC mode. $H_{EB}(T)$ and $H_C(T)$ exhibit a monotonic decrease upon increasing temperature, which is for $H_C(T)$ interrupted by a local maximum around 40 K. The origin of this anomaly will be discussed later.

We will now turn our focus to the details of the magnetic phase diagram of Mn_2PtGa. Figure 3 displays the ZFC $M(H)$ loops at various temperatures. The 10 K $M(H)$ loop shows a similar behavior as that at 1.9 K [Fig. 1(c)] with a reduction of the field required to induce the metamagnetic transition. Interestingly, the metamagnetic transition is only observed in the virgin curve for $T \leq 15$ K. However, at 17.5 K the loop shows a signature of the metamagnetic transition in the negative field path. Upon increasing temperature this signature becomes more pronounced for negative as well as positive fields. The presence of the virgin curve outside the envelope loop and the

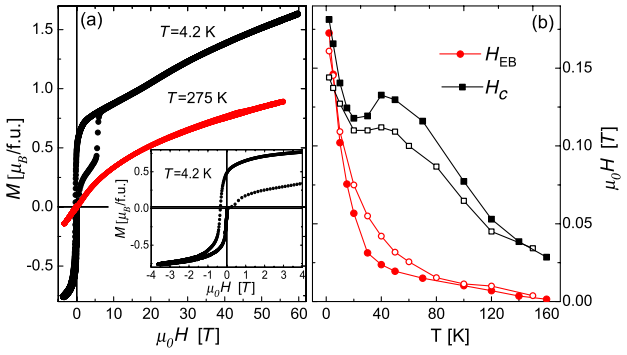

FIG. 2 (color online). (a) $M(H)$ isotherms at 4.2 and 275 K in fields up to 60 T. Inset: Data at 4.2 K in the low field range. (b) $H_{EB}(T)$ and $H_C(T)$ taken from the ZFC (closed symbols) and FC (open symbols) $M(H)$ isotherms.

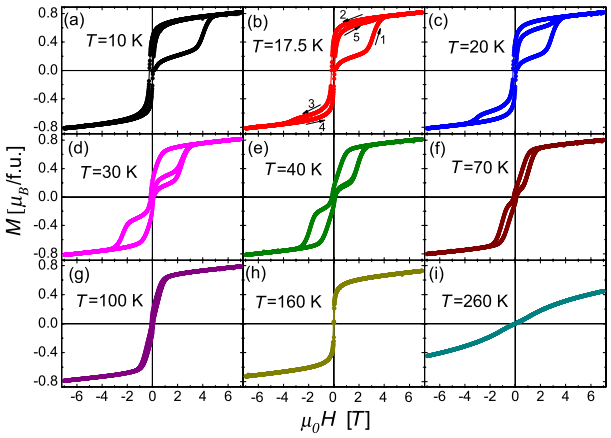

FIG. 3 (color online). ZFC $M(H)$ loops taken at different T.

incomplete metamagnetic transition results in an irreversible hysteresis loop for $T < 40$ K. The $M(H)$ loops for $T \geq 40$ K are reversible in both quadrants, also the virgin curve coincides with the corresponding part of the hysteresis loop. The critical field of the metamagnetic transition decreases significantly upon increasing temperature. The feature of the metamagnetic transition completely vanishes at 160 K, where we find soft FM behavior and finally a paramagnetic $M(H)$ loop at 260 K. However, the loops remain shifted in the negative field direction for $T \leq 160$ K. From the above observations we can divide the whole temperature range into different intervals: $0 < T \leq 15$ K, the AFM phase, which was converted to FI, cannot be recovered by any number of field cycling. This results in a large field-induced irreversibility in the $M(H)$ loops. In the temperature range $15 < T < 40$ K, the AFM phase can be partially restored. At higher temperatures ($40 < T < 150$ K), the AFM phase that was initially converted to the FI phase is recovered fully to its initial state by cycling the magnetic field. Here the hysteresis loops are fully reversible and the AFM phase returns to its initial state by reducing the field to zero. The peak in $H_C(T)$ around 40 K, shown in Fig. 2(b), originates from the irreversible hysteresis loops in the range of $17.5 \leq T \leq 40$ K. This results in a nominal increase of $H_C(T)$ upon increasing temperature for $17.5 \leq T \leq 40$ K followed by a reduction for reversible loops at higher temperatures.

The disorder influenced first-order magnetic to magnetic transition in Mn_2PtGa is found for the first time in any Heusler compound. The observation of different magnitudes of field-induced irreversibility is a direct consequence of the competition between the potential and thermal energy. Though the AFM phase possesses a lower energy at $H = 0$ for $T \leq 15$ K, the field-induced FI phase forms a pinning potential, where disorder provides the pinning centers. When the field is reduced to zero, the thermal energy cannot overcome this potential and the AFM phase is not restored, resulting in the observed irreversibilities. At higher temperatures the thermal energy becomes large enough to allow for a partial recovery of the AFM phase by field cycling. Only above 40 K the thermal energy becomes larger than the pinning potential and a reversible hysteresis loop is observed. Similar phenomena have been reported in systems undergoing a first-order magnetic to magnetic transition [22,23]. Although some of the Heusler systems with martensitic transition show a similar type of field-induced irreversibility, the underlying physics for such a behavior categorically differs from the case of Mn_2PtGa. In the former materials the field-induced structural change plays a major role in inducing the irreversibilities, which become stronger on approaching the martensitic transition upon increasing temperature [24,25]. This is in contrast to Mn_2PtGa which does not show any structural transition.

To map out the exact magnetic configuration in Mn_2PtGa, we have performed calculations using the fully relativistic linearized muffin-tin orbitals band-structure method within the PYA-LMTO program package [20]. The unit cell parameters were taken from experiment. The exchange-correlation potential was treated using the Vosko-Wilk-Nusair form of the local density approximation [26]. The comparison of the total energy calculated for the different configurations (see Fig. 4) indicates that the nonmagnetic configurations are energetically the most unfavorable (regular and inverse variants). The energy is substantially reduced by switching on the magnetism on the Mn atoms. For a ferromagnetic configuration this results in a large magnetic moment: 7.2 μ_B/f.u. in the case of the regular and 7.12 μ_B/f.u. for the inverse

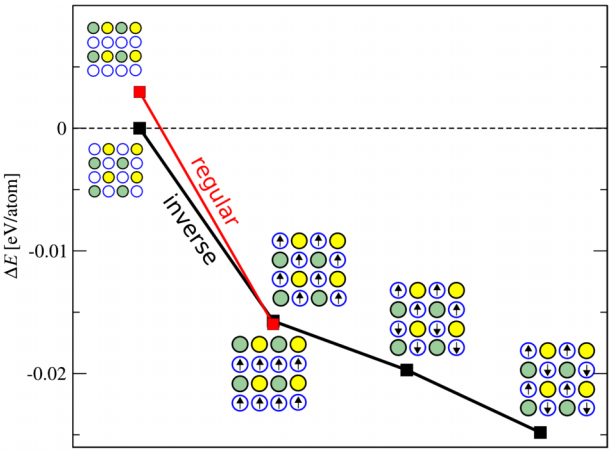

FIG. 4 (color online). Total energies for various magnetic configurations in the case of inverse (black line) and regular (red line) Heusler structures. The energy of the inverse Heusler structure in the nonmagnetic state is taken as reference. The chemical composition of each configuration is schematically depicted by the (4×4)-atom diagrams drawn closer to the corresponding energy points. Gray (light green), light gray (yellow), and hollow spheres mark Pt, Ga, and Mn atoms, respectively. Arrows on Mn spheres indicate the directions of the local magnetic moments.

Heusler structure. In this fully ferromagnetic setup both regular and inverse structures possess rather similar total energies of about -15 meV/atom compared with the nonmagnetic inverse structure. For the regular Heusler variant the ferromagnetic state is the most stable. Enforcing any type of antiparallel alignment of Mn moments within the regular structure always leads to a locally nonmagnetic state. On the other hand, by varying the magnetic configurations further within the inverse structure, the total energy can still be lowered. By reverting the directions of the magnetic moments in each second pair of layers, we arrive in the fully compensated antiferromagnetic state, with an energy lowered by about 4 meV/atom compared with the ferromagnetic state. The lowest energy configuration is achieved when the Mn moment is reverted within each layer (FI state). Since the positions of the Mn atoms in the adjacent layers within the inverted Heusler structure are nonequivalent by symmetry, the total magnetic moment is not completely compensated: a small total moment of about 0.55 μ_B/f.u., which is the result of 3.65 μ_B/f.u.[Mn(I)] $-$ 3.1 μ_B/f.u.[Mn(II)], remains. Our results emphasize that the formation of the magnetic state is driven by two mechanisms: ferromagnetic exchange between Mn atoms at long and antiferromagnetic at short distances.

The observation of a magnetization of 0.8 μ_B/f.u. at 7 T is slightly larger than the calculated value (0.55 μ_B/f.u.). This can be explained by ferromagnetic clusters embedded in the strongly compensated ferrimagnetic host. The ferromagnetic ordering inside the clusters is due to their regular Heusler structure, i.e., the interchange between Mn and Pt atoms (the so-called antisite disorder, which often takes place in Heusler materials). Samples prepared under different annealing and/or quenching conditions exhibit a slightly changed magnetization. This is most likely connected to an atomic rearrangement toward the more stable, inverse Heusler structure. The latter phase forms an almost compensated host, which surrounds the ferromagnetic clusters.

Based on the first-principles calculations and experimental results, we propose a simple model for the ZFC EB in Mn_2PtGa. We assume an exchange interaction between two dissimilar magnetically anisotropic phases. The irreversibility between ZFC and FC $M(T)$ curves in low fields (≤ 0.1 T), the frequency dependence of $\chi''(T)$ below T_C, and the theoretical calculations indicate the presence of magnetically inhomogeneous states originating from local FM clusters in a FI background. Upon applying field the virgin magnetization process will try to align the moments in the FI and FM phases along the field direction, which implies that the interface spins of the FI and FM phases will align in the same direction to minimize the energy. This sets up the exchange interaction between the magnetically soft FM phase and the magnetically hard FI phase. Further, this implies an increase of the coercive field in a perfectly ordered material, because the ferrimagnetically ordered moments collectively change their direction [27]. However, one would expect a rough interface with disorder and uncompensated moments in the FI phase and additional defects in the bulk [27–29]. All of these factors collectively contribute to the ZFC EB behavior. The fact that H_{EB} obtained from the FC $M(H)$ loops measured after field cooling in 7 T, where the sample is only in the FI phase below T_C, and the H_{EB} derived from the ZFC loops almost match rules out any significance of the first-order FI to AFM transition in the formation of the ZFC EB. This is furthermore supported by the observation of a small EB at 160 K, which is above the FI to AFM transition. The pulsed field experiments up to 60 T find only a very small change in H_{EB}. This shows that, once the exchange interaction is set up, the field does not change the FI phase significantly to observe a change in H_{EB}. These findings distinguish Mn_2PtGa from the off-stoichiometric Ni-Mn-In Heusler alloys where recently a ZFC EB has been reported [8]. Mn_2PtGa exhibits a too weak frequency dependence of the peak in $\chi''(T)$ to indicate super spin-glass behavior resulting in super FM clusters during the initial magnetization process as in Ni-Mn-In [8]. One common factor, however, is the existence of FI ordering in both systems. Therefore, we argue that the presence of FI ordering with embedded FM clusters is an important ingredient for the appearance of a ZFC EB.

In conclusion, we have synthesized and studied the new Heusler compound Mn_2PtGa. Even though Mn_2PtGa orders ferrimagnetically at $T_C = 230$ K, it undergoes an unusual first-order FI to AFM phase transition below T_C. We demonstrated, to our knowledge for the first time, the presence of a ZFC EB effect in a stoichiometric bulk Heusler compound. We further show that the appearance of this ZFC EB effect is related to the presence of FI ordering with embedded FM clusters. We ruled out any role of the first-order transition in the observation of the ZFC EB.

We thank J. A. Mydosh for valuable discussions on the present work. This work was financially supported by the Deutsche Forschungsgemeinschaft DFG (Projects No. TP 1.2-A and No. 2.3-A of Research Unit FOR 1464 ASPIMATT) and by the ERC Advanced Grant No. (291472) ''Idea Heusler.'' The experiments at the High Magnetic Field Laboratory Dresden (HLD) were sponsored by Euro-MagNET II under the European Union Contract No. 228043.

*nayak@cpfs.mpg.de
†nicklas@cpfs.mpg.de

[1] T. Krenke, E. Duman, M. Acet, E. F. Wassermann, X. Moya, L. Mañosa, and A. Planes, Nat. Mater. **4**, 450 (2005).
[2] R. Kainuma, Y. Imano, W. Ito, Y. Sutou, H. Morito, S. Okamoto, O. Kitakami, K. Oikawa, A. Fujita,

T. Kanomata, and K. Ishida, Nature (London) **439**, 957 (2006).
[3] J. Liu, T. Gottschall, K. P. Skokov, J. D. Moore, and O. Gutfleisch, Nat. Mater. **11**, 620 (2012).
[4] M. Pasquale, C. P. Sasso, L. H. Lewis, L. Giudici, T. Lograsso, and D. Schlagel, Phys. Rev. B **72**, 094435 (2005).
[5] J. Enkovaara, O. Heczko, A. Ayuela, and R. M. Nieminen, Phys. Rev. B **67**, 212405 (2003).
[6] S. Aksoy, M. Acet, P. P. Deen, L. Mañosa, and A. Planes, Phys. Rev. B **79**, 212401 (2009).
[7] T. Graf, C. Felser, and S. S. P. Parkin, Prog. Solid State Chem. **39**, 1 (2011).
[8] B. M. Wang, Y. Liu, P. Ren, B. Xia, K. B. Ruan, J. B. Yi, J. Ding, X. G. Li, and L. Wang, Phys. Rev. Lett. **106**, 077203 (2011).
[9] S. Chatterjee, S. Giri, S. K. De, and S. Majumdar, Phys. Rev. B **79**, 092410 (2009).
[10] A. K. Nayak, K. G. Suresh, and A. K. Nigam, J. Phys. Condens. Matter **23**, 416004 (2011).
[11] M. Khan, I. Dubenko, S. Stadler, and N. Ali, Appl. Phys. Lett. **91**, 072510 (2007).
[12] S. Mizukami, F. Wu, A. Sakuma, J. Walowski, D. Watanabe, T. Kubota, X. Zhang, H. Naganuma, M. Oogane, Y. Ando, and T. Miyazaki, Phys. Rev. Lett. **106**, 117201 (2011).
[13] B. Balke, G. H. Fecher, J. Winterlik, and C. Felser, Appl. Phys. Lett. **90**, 152504 (2007).
[14] J. Winterlik, B. Balke, G. H. Fecher, C. Felser, M. C. M. Alves, F. Bernardi, and J. Morais, Phys. Rev. B **77**, 054406 (2008).
[15] H. Kurt, K. Rode, M. Venkatesan, P. S. Stamenov, and J. M. D. Coey, Phys. Rev. B **83**, 020405(R) (2011).
[16] J. Winterlik, G. H. Fecher, B. Balke, T. Graf, V. Alijani, V. Ksenofontov, C. A. Jenkins, O. Meshcheriakova, C. Felser, G. Liu, S. Ueda, K. Kobayashi, T. Nakamura, and M. Wójcik, Phys. Rev. B **83**, 174448 (2011).
[17] P. Klaer, C. A. Jenkins, V. Alijani, J. Winterlik, B. Balke, C. Felser, and H. J. Elmers, Appl. Phys. Lett. **98**, 212510 (2011).
[18] A. K. Nayak, C. Shekhar, J. Winterlik, A. Gupta, and C. Felser, Appl. Phys. Lett. **100**, 152404 (2012).
[19] See Supplemental Material at http://link.aps.org/supplemental/10.1103/PhysRevLett.110.127204 for details of the sample characterization.
[20] S. H. Vosko, L. Wilk, and M. Nusair, Can. J. Phys. **58**, 1200 (1980).
[21] S. B. Roy, G. K. Perkins, M. K. Chattopadhyay, A. K. Nigam, K. J. S. Sokhey, P. Chaddah, A. D. Caplin, and L. F. Cohen, Phys. Rev. Lett. **92**, 147203 (2004).
[22] K. Sengupta and E. V. Sampathkumaran, Phys. Rev. B **73**, 020406(R) (2006).
[23] J. Dho and N. H. Hur, Phys. Rev. B **67**, 214414 (2003).
[24] V. K. Sharma, M. K. Chattopadhyay, and S. B. Roy, Phys. Rev. B **76**, 140401(R) (2007).
[25] A. K. Nayak, K. G. Suresh, and A. K. Nigam, Appl. Phys. Lett. **96**, 112503 (2010).
[26] A. Perlov, A. Yaresko, and V. Antonov (unpublished).
[27] J. Nogués, J. Sort, V. Langlais, V. Skumryev, S. Suriñach, J. S. Muñoz, and M. D. Baró, Phys. Rep. **422**, 65 (2005).
[28] J. Nogués and I. K. Schuller, J. Magn. Magn. Mater. **192**, 203 (1999).
[29] M. Kiwi, J. Magn. Magn. Mater. **234**, 584 (2001).